Eur. Phys. J. C 28, 329–333 (2003)
Digital Object Identifier (DOI) 10.1140/epjc/s2003-01187-3

THE EUROPEAN PHYSICAL JOURNAL C

Experimental tests of non-perturbative pion wave functions

D. Ashery[1,a], H.-C. Pauli[2,b]

[1] School of Physics and Astronomy, Raymond and Beverly Sackler Faculty of Exact Sciences, Tel Aviv University, Israel
[2] Max-Planck-Institut für Kernphysik, 69029 Heidelberg, Germany

Received: 15 January 2003 /
Published online: 14 April 2003 –

Abstract. We use the transverse-momentum dependence of the cross section for the diffractive dissociation of high energy pions to two jets to study some non-perturbative light-cone wave functions of the pion. We compare the predictions for this distribution by Gaussian and Coulomb wave functions as well as the wave function derived from a solution of the light-cone Hamiltonian in the singlet model. We conclude that this experimentally measured information provides a powerful tool for these studies.

1 Light-cone wave functions

One of the most interesting subjects of particle and nuclear physics is understanding the internal structure of hadrons. It bears directly on the fundamental interactions of the quarks and gluons that create the hadronic bound state. It is also an essential ingredient in understanding the hadronic strong, electromagnetic and weak interactions. A very powerful description of the hadronic structure is obtained through the light-cone wave functions. These are frame-independent and process-independent quantum-mechanical descriptions at the amplitude level. They encode all possible quark and gluon momentum, helicity and flavor correlations in the hadron. The light-cone wave functions are constructed from the QCD light-cone Hamiltonian [1] $H_{\rm LC}^{\rm QCD} = P^+P^- - P_\perp^2$, where $P^\pm = P^0 \pm P^z$. The wave function ψ_h for a hadron h with mass M_h satisfies the relation $H_{\rm LC}^{\rm QCD}|\psi_h\rangle = M_h^2|\psi_h\rangle$.

The light-cone wave functions are expanded in terms of a complete basis of Fock states having increasing complexity. In this way the hadron presents itself as an ensemble of coherent states containing various numbers of quark and gluon quanta [2]. For example, the negative pion has the Fock expansion

$$|\psi_{\pi^-}\rangle = \sum_n \langle n|\pi^-\rangle|n\rangle = \psi^{(\Lambda)}_{d\bar{u}/\pi}(u_i, \mathbf{k}_{\perp i})|\bar{u}d\rangle + \psi^{(\Lambda)}_{d\bar{u}g/\pi}(u_i, \mathbf{k}_{\perp i})|\bar{u}dg\rangle + \ldots$$

representing the expansion of the exact QCD eigenstate at scale Λ in terms of non-interacting quarks and gluons. They have longitudinal light-cone momentum fractions:

$$u_i = \frac{k_i^+}{p^+} = \frac{k_i^0 + k_i^z}{p^0 + p^z}\ , \qquad \sum_{i=1}^n u_i = 1\ , \tag{1}$$

and relative transverse momenta

$$\mathbf{k}_{\perp i}\ , \qquad \sum_{i=1}^n \mathbf{k}_{\perp i} = \mathbf{0}_\perp\ . \tag{2}$$

The form of $\psi_{n/H}(u_i, \mathbf{k}_{\perp i})$ is invariant under longitudinal and transverse boosts; i.e., the light-cone wave functions expressed in the relative coordinates u_i and $k_{\perp i}$ are independent of the total momentum (p^+, $\mathbf{p}_\perp$) of the hadron. The Fock states are off mass shell with masses of $M_n = \sum_{i=1}^n (k_{\perp i}^2 + m_i^2)/u_i$, where m_i are the quark (current) masses. The first term in the expansion is referred to as the valence Fock state, as it relates to the hadronic description in the constituent quark model. The higher terms are related to the sea components of the hadronic structure. It has been shown that once the valence Fock state is determined it is possible to build the rest of the light-cone wave function [3,4]. This was done for the pion using discretized light-cone quantization (DLCQ) on a transverse lattice [5,6].

The hadronic distribution amplitude $\phi(u, Q^2)$ is the probability amplitude to find a quark and an antiquark of the respective lowest-order Fock state carrying fractional momenta u and $1-u$ [7,8]. The pion distribution amplitude and the light-cone wave function of the respective Fock state ψ are related through [7,8]

$$\phi_{q\bar{q}/\pi}(u, Q^2) \sim \int_0^{Q^2} \psi_{q\bar{q}/\pi}(u, \tilde{k_\perp^2})\mathrm{d}^2\tilde{k_\perp}\ , \tag{3}$$

$$Q^2 = \frac{k_\perp^2}{u(1-u)}\ . \tag{4}$$

Two functions have been proposed to describe the momentum distribution amplitude for the quark and antiquark in

[a] e-mail: ashery@tauphy.tau.ac.il
[b] e-mail: pauli@mpi-hd.mpg.de

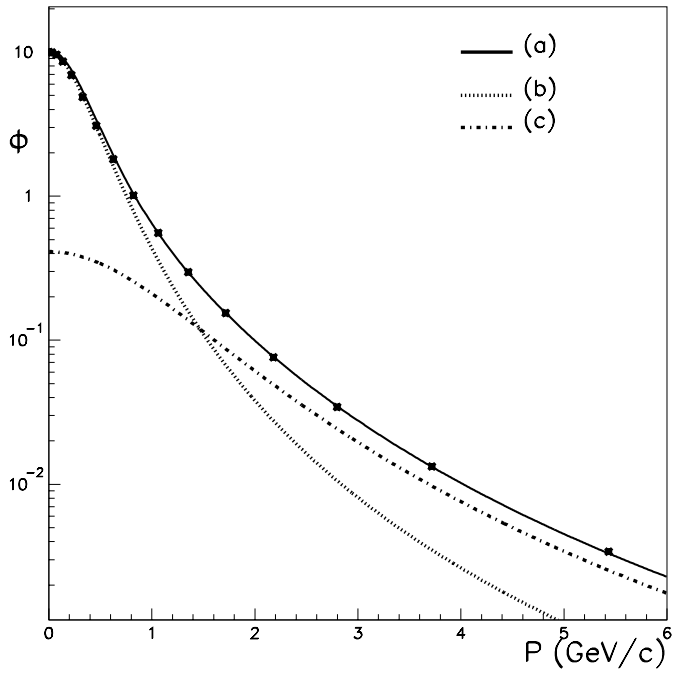

Fig. 1. Fits to the singlet-model wave function. (a) is the fit to the full range, (b) is the fit to the low range first term, and (c) is the fit to the higher range, second term. The resulting parameters are $a = 0.7$, $p_a = 0.515\,\mathrm{GeV}/c$, $b = 2.55$, $p_b = 1.58\,\mathrm{GeV}/c$

the $|q\bar{q}\rangle$ configuration. The asymptotic function was calculated using perturbative QCD (pQCD) methods [7–11] and is the solution to the pQCD evolution equation for very large Q^2 ($Q^2 \to \infty$):

$$\phi_{as}(u) = \sqrt{3}u(1-u)\,. \tag{5}$$

Using QCD sum rules, Chernyak and Zhitnitsky (CZ) [12] proposed a function that is expected to be correct for low Q^2:

$$\phi_{\mathrm{cz}}(u) = 5\sqrt{3}u(1-u)(1-2u)^2\,. \tag{6}$$

In recent experimental work [13] it was concluded that the asymptotic distribution amplitude describes the pion well for $Q^2 > 10\,(\mathrm{GeV}/c)^2$; see also Fig. 2b.

Alternative approaches are based directly on the wave function, particularly for the non-perturbative low Q^2-region. Jakob and Kroll [14] proposed a Gaussian function: $\psi \sim \mathrm{e}^{-\beta k_\perp^2}$. Pauli [15] considers the $L_z = S_z = 0$ component of the $u\bar{d}$ wave function in the singlet model: $\psi(u, \mathbf{k}_\perp) \equiv \Psi_{u\bar{d}}(u, \mathbf{k}_\perp; \uparrow\downarrow)$. Then $H_{\mathrm{LC}}^{\mathrm{QCD}}|\psi_h\rangle = M_h^2|\psi_h\rangle$ translates to (8) of [15]:

$$M^2\psi(u,\mathbf{k}_\perp) = \frac{m^2+\mathbf{k}_\perp^2}{u(1-u)}\;\psi(u,\mathbf{k}_\perp) - \frac{\alpha}{3\pi^2}\int\frac{\mathrm{d}u'\mathrm{d}^2\mathbf{k}'_\perp\;\psi(u',\mathbf{k}'_\perp)}{\sqrt{u(1-u)u'(1-u')}}\left(\frac{4m^2}{Q^2}+\frac{2\mu^2}{\mu^2+Q^2}\right)\,, \tag{7}$$

for equal masses $m_1 = m_2 = m$, and for the mean Feynman four-momentum transfer Q^2 of the quarks. Replacing the integration variable u by k_z we have accordingly

$$u = \frac{1}{2}\left[1 + \frac{k_z}{\sqrt{m^2+\mathbf{k}_\perp^2+k_z^2}}\right]\,. \tag{8}$$

Inversely, one expresses k_z by u with

$$k_z^2 = (m^2+\mathbf{k}_\perp^2)\;\frac{\left(u-\frac{1}{2}\right)^2}{u(1-u)}\,. \tag{9}$$

The substitution allows us to introduce the 3-vector $\mathbf{p} \equiv (\mathbf{k}_\perp, k_z)$ and to transscribe this integral equation into

$$\left[4m^2+4\mathbf{p}^{\,2}\right]\varphi(\mathbf{p}) - \frac{2\alpha}{3\pi^2}\int\frac{\mathrm{d}^3\mathbf{p}'\;\varphi(\mathbf{p}')}{m\sqrt{A(p)A(p')}}\left(\frac{4m^2}{Q^2}+\frac{2\mu^2}{\mu^2+Q^2}\right) = M^2\varphi(\mathbf{p})\,. \tag{10}$$

This equation was numerically solved for $\varphi(\mathbf{p})$ [15], in the non-relativistic approximation $A(p) = \sqrt{1+\mathbf{p}^2/m^2} \sim 1$. In this approximation, the mean four-momentum becomes $Q^2 = (\mathbf{p}-\mathbf{p}')^2$, and the light-cone wave function $\psi(u, \mathbf{k}_\perp)$ is related to the reduced wave function $\varphi(k_z, \mathbf{k}_\perp)$ by

$$\psi(u,\mathbf{k}_\perp) = \frac{\varphi(k_z,\mathbf{k}_\perp)}{\sqrt{u(1-u)}}\;; \tag{11}$$

for details see [15]. The parameters $\alpha = 0.69$, $m = 0.406\,\mathrm{GeV}$ and $\mu = 1.33\,\mathrm{GeV}$ yield the correct mass-squared eigenvalue $M^2 = (140\,\mathrm{MeV})^2$ for the pion and all other isoscalar mesons.

The isotropic numerical wave function $\varphi(\mathbf{p})$ is parametrized [16,17] for $p < 0.9\,\mathrm{GeV}/c$ by

$$\varphi(\mathbf{p}) = \frac{\mathcal{N}}{\left(p_a^2+\mathbf{p}^{\,2}\right)^2}, \qquad p_a = 0.515\,\mathrm{GeV}/c\,, \tag{12}$$

that is, like a Coulomb wave function with an abnormally large Bohr momentum: $p_a > m$. In Fig. 1 we present a parametrization of the full range of the calculated wave function [17] by a two-term Coulomb wave function. The first term is kept as in (12) with $p_a = 0.515\,\mathrm{GeV}/c$. The mean momentum of the second term, p_b, and the two normalization constants a, b are free parameters:

$$\varphi(\mathbf{p}) = \frac{a}{\left(p_a^2+\mathbf{p}^{\,2}\right)^2} + \frac{b}{\left(p_b^2+\mathbf{p}^{\,2}\right)^2}\,. \tag{13}$$

By extending the parametrization to the higher momentum range we can expect this function to be relevant to the measured $k_\perp$-distribution.

The light-cone wave function (11) with the variable transform (9) becomes

$$\psi(u,\mathbf{k}_\perp) = 2\mathcal{N}\left[\frac{a\,[4u(1-u)]^{\frac{3}{2}}}{\left[\mathbf{k}_\perp^2+K_a^2(u)\right]^2} + \frac{b\,[4u(1-u)]^{\frac{3}{2}}}{\left[\mathbf{k}_\perp^2+K_b^2(u)\right]^2}\right]\,,$$

with

$$K_a^2(u) = 4u(1-u)p_a^2 + (2u-1)^2m^2\,,$$
$$K_b^2(u) = 4u(1-u)p_b^2 + (2u-1)^2m^2\,. \tag{14}$$

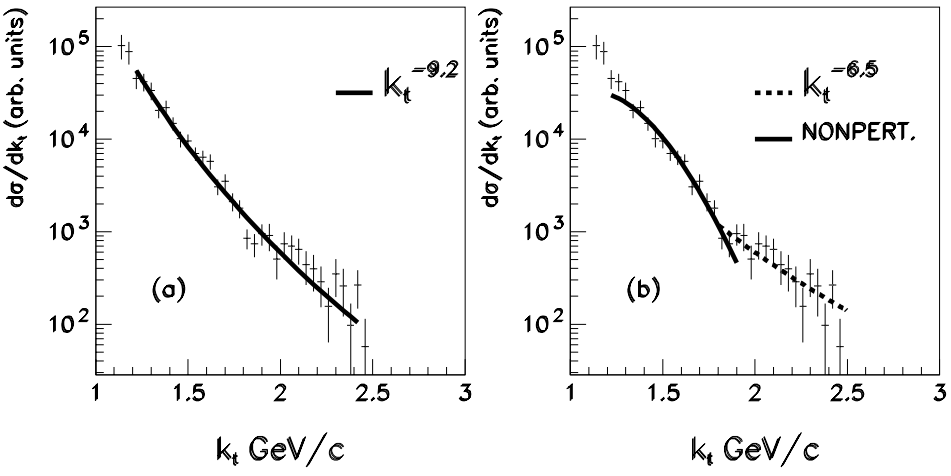

Fig. 2a,b. Comparison of the k_t-distribution of acceptance corrected data with fits to cross section dependence **a** according to a power law, **b** based on a non-perturbative Gaussian wave function for low k_t and a power law, as expected from perturbative calculations, for high k_t. Reproduced from [13]

The main experimental test of the wave function in the non-perturbative regime has traditionally been through measurements of the pion electromagnetic form factor [18]. However, as shown by the authors, there is little sensitivity of the form factor to the distribution function. It is therefore desirable to develop alternative ways for these tests.

2 Measurement of the light-cone wave function

The recent measurement of the pion light-cone wave function [13] is based on the following concept: a high energy pion dissociates diffractively on a heavy nuclear target. The first (valence) Fock component dominates at large Q^2; the other terms are suppressed by powers of $1/Q^2$ for each additional parton, according to counting rules [18, 19]. This is a coherent process in which the quark and antiquark break apart and hadronize into two jets. If in this fragmentation process the quark momentum is transferred to the jet, measurement of the jet momentum gives the quark (and antiquark) momentum. The proportionality of the differential cross section with respect to the jet momentum to the distribution amplitude (squared) was asserted [20]:

$$\frac{\mathrm{d}^3\sigma_N}{\mathrm{d}u\,\mathrm{d}M_J^2\cdot\mathrm{d}^2P_{N_t}} = 2.6\,\mathrm{GeV}^{-6}\left(\frac{\mathrm{GeV}}{\kappa_t}\right)^8\phi^2(u), \qquad (15)$$

and

$$u_{\mathrm{measured}} = \frac{p_{\mathrm{jet1}}}{p_{\mathrm{jet1}}+p_{jet2}}\ .$$

k_t is the measured transverse momentum of each jet. It is assumed that $k_t(\mathrm{jet}) \sim k_\perp(\mathrm{quark})$. This relation was also studied via Monte Carlo simulations in order to verify the proportionality and take into account smearings in the fragmentation process and kinematic effects [13]. From simple kinematics and assuming that the masses of the jets are small compared with the mass of the di-jets, the virtuality and mass-squared of the di-jets are given by

$$Q^2 \sim M_{\mathrm{DJ}}^2 = \frac{k_t^2}{u(1-u)}\ .$$

The results of the measurement show that for $k_t > 1.5\,\mathrm{GeV}/c$, which translates to $Q^2 > 10\,(\mathrm{GeV}/c)^2$, there is good agreement between the data and the asymptotic wave function. The conclusion was that the pQCD approach that led to construction of the asymptotic wave function is reasonable for $Q^2 > 10\,(\mathrm{GeV}/c)^2$. At lower values contributions from non-perturbative effects may become noticeable. In this work we focus our attention to this transition region.

3 The k_t-distribution

The k_t-dependence of diffractive di-jets is another observable that can show how well the various wave functions describe the data. As shown in [20] this dependence is expected to be $\frac{\mathrm{d}\sigma}{\mathrm{d}k_t} \sim k_t^{-6}$ for one gluon exchange perturbative calculations. The experimental results are shown in Fig. 2, reproduced from [13]. In Fig. 2a the results were fitted by k_t^n for $k_t > 1.25\,\mathrm{GeV}$ with $n = -9.2 \pm 0.5$. This slope is significantly larger than expected. However, the region above $k_t \sim 1.8\,\mathrm{GeV}/c$ could be fitted (Fig. 2b) with $n = -6.5 \pm 2.0$, consistent with the predictions. This would support the evaluation of the light-cone wave function at large k_t as due to one gluon exchange, as is the asymptotic wave function.

The lower k_t-region can be considered as a transition from the perturbative to the non-perturbative regimes. The experimental results go down to $k_t \sim 1\,\mathrm{GeV}/c$, still large if we want to consider it as a fully non-perturbative regime. In [13] this region was fitted with the non-perturbative Gaussian function: $\psi \sim \mathrm{e}^{-\beta k_t^2}$ [14], resulting in $\beta = 1.78 \pm 0.1$. Model-dependent values in the range of 0.9–4.0 were used [14]. This fit, although resulting in the parameter β being consistent with theoretical expectations, is not very satisfactory. As seen in Fig. 2b the curved shape of the theoretical calculation is not observed in the data.

We now turn to a comparison of the experimental data with the prediction of the wave function based on the singlet model (Sect. 1). For this purpose we begin with the same expression used by the authors of [13],

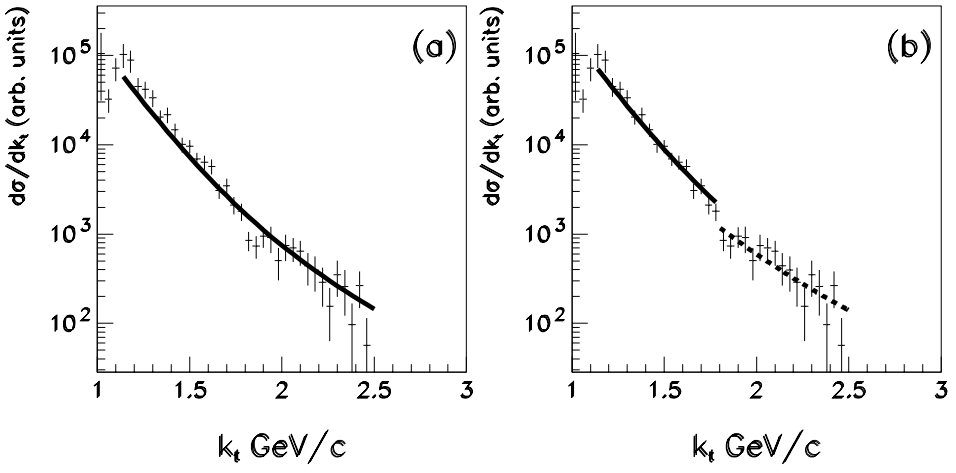

Fig. 3a,b. Comparison of the k_t-distribution of acceptance corrected data with fits to the cross section derived from **a** the two-terms wave function representing the full range of the singlet-model wave function. **b** The two-term wave function for low k_t, and a power law, as expected from perturbative calculations, for high k_t

$$\frac{\mathrm{d}\sigma}{\mathrm{d}k_t^2} \propto \left|\alpha_\mathrm{s}(k_t^2)G(u,k_t^2)\right|^2 \left|\frac{\partial^2}{\partial k_t^2}\psi(u,k_t)\right|^2 , \qquad (16)$$

with $\alpha_\mathrm{s}(k_t^2)G(u,k_t^2) \sim k_t^{\frac{1}{2}}$, which is based on factorization and which actually is a double differential cross section. Using it with the ψ from (14) gives

$$\frac{\mathrm{d}^2\sigma}{\mathrm{d}u\;\mathrm{d}k_T} = \mathcal{N}_1\;\frac{[4u(1-u)]^3}{k_t^{10}}\frac{\left[1-\frac{1}{2}\dfrac{K_a^2(u)}{k_t^2}\right]^2}{\left[1+\quad\dfrac{K_a^2(u)}{k_t^2}\right]^8} , \qquad (17)$$

up to a constant $\mathcal{N}_1$, and up to similar terms with K_b^2.

The k_t-distribution is obtained from (17) as a single differential cross section by integrating over u. But since $\mathrm{d}^2\sigma/\mathrm{d}u\;\mathrm{d}k_t$ is strongly peaked at $u=\frac{1}{2}$, an exact treatment is both complicated and unnecessary. Rather, it is approximated by removing the slowly varying terms from the integral,

$$\frac{\mathrm{d}\sigma}{\mathrm{d}k_t} = \frac{\mathcal{N}_1}{k_t^{10}}\frac{\left[1-\frac{1}{2}\dfrac{\langle K_a^2\rangle}{k_t^2}\right]^2}{\left[1+\quad\dfrac{\langle K_a^2\rangle}{k_t^2}\right]^8}\int_0^1 \mathrm{d}u\,[u(1-u)]^3 , \qquad (18)$$

and similarly for the b-terms. The average value $\langle K_a^2\rangle$ is evaluated in two different approximations:

$$\langle K_a^2\rangle = p_a^2 , \qquad (19)$$

and

$$\langle K_a^2\rangle = \frac{8}{9}p_a^2 + \frac{1}{9}m^2 , \qquad (20)$$

and similarly for the b-terms. The former is obtained by the peak value $\langle K_a^2\rangle = K_a^2\left(\frac{1}{2}\right)$, the latter is obtained by the weighted average

$$\langle u(1-u)\rangle = \frac{\int_0^1 \mathrm{d}u\;w(u)\;u(1-u)}{\int_0^1 \mathrm{d}u\;w(u)} = \frac{2}{9} , \qquad (21)$$

$$\langle (2u-1)^2\rangle = \frac{\int_0^1 \mathrm{d}u\,w(u)\;(2u-1)^2}{\int_0^1 \mathrm{d}u\;w(u)} = \frac{1}{9} , \qquad (22)$$

with the weight function $w(u) = [u(1-u)]^3$. For the particular case $p_a = m$ both approximations coincide.

In Fig. 3a we compare the prediction of (19) with the data over the whole measured range. Only the total normalization constant $\mathcal{N}_1$ is a free parameter. The quality of the fit ($\chi^2 = 1.7$) improves significantly when we repeat the fit only in the low k_t-region ($\chi^2 = 0.8$). This is shown in Fig. 3b with the higher k_t range left as in Fig. 2b.

4 The u-distributions

Finally, we consider the u-dependence of the diffractive di-jets by integrating the double differential cross section (17) over the transverse momentum k_t. E791 [13] measures conditional u-distributions

$$\left.\frac{\mathrm{d}\sigma}{\mathrm{d}u}\right|_{(k_l,k_u)} , \qquad \text{with} \quad k_l \le k_t \le k_u , \qquad (23)$$

for the momentum intervals $1.25\,\mathrm{GeV}/c \le k_t \le 1.5\,\mathrm{GeV}/c$ and $1.5\,\mathrm{GeV}/c \le k_t \le 2.\,\mathrm{GeV}/c$. For comparing that with theory one should integrate (17), and we do this in terms of the auxiliary function $G(u) = G(u;k_l)$:

$$G(u;k_l) \equiv \int \mathrm{d}^2k_t\;\frac{\mathrm{d}^2\sigma}{\mathrm{d}u\;\mathrm{d}k_t}\;\theta(k_t^2-k_l^2) \qquad (24)$$
$$= \pi\mathcal{N}_1\,[u(1-u)]^3\int_{k_l^2}^{\infty}\mathrm{d}z\;z\;\frac{\left[z-\frac{1}{2}K_a^2(u)\right]^2}{\left[z+\quad K_a^2(u)\right]^8} .$$

The integration can be carried out analytically:

$$G(u;k_l) = \pi\mathcal{N}_1\frac{[u(1-u)]^3}{\left[k_l^2+K_a^2(u)\right]^7} \qquad (25)$$
$$\times\left[\frac{k_l^6}{4} - \frac{k_l^4}{20}K_a^2(u) + \frac{k_l^2}{40}K_a^4(u) + \frac{1}{280}K_a^6(u)\right] .$$

The conditional u-distributions then become

$$\left.\frac{\mathrm{d}\sigma}{\mathrm{d}u}\right|_{(k_l,k_u)} = G(u;k_l) - G(u;k_u) . \qquad (26)$$

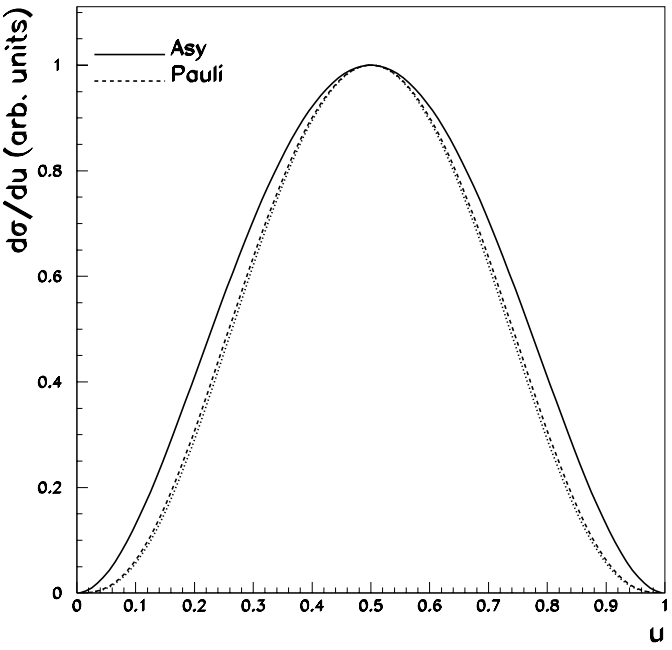

Fig. 4. The asymptotic distribution $[u(1-u)]^2$ (solid line) is compared with two u-distributions calculated for $1.25\,\mathrm{GeV}/c \leq k_t \leq 1.5\,\mathrm{GeV}/c$, and $1.5\,\mathrm{GeV}/c \leq k_t \leq 2.5\,\mathrm{GeV}/c$ which almost coincide (dashed lines). All curves are normalized at $u = 0.5$

In Fig. 4 we compare the predictions of (26) to the asymptotic distribution $[u(1-u)]^2$ of [7–11]. Only the overall normalization is used as free parameter. They are narrower than $[u(1-u)]^2$ mostly due to the factor $[u(1-u)]^3$ in (24).

5 Discussion and conclusions

The agreement of the calculated k_t-distribution with the data in the transition region of Fig. 3 is interesting since the wave function is a non-perturbative solution of a relatively simple model for the light-cone Hamiltonian. The model was developed for the bound state problem in physical mesons [15], where the low $k_\perp$-properties are important. It is surprising that this model describes also the large $k_\perp$-properties in the tail of the wave function; without that a re-fit of the parameters is necessary.

The non-relativistic approximation to (10) predicts a u-distribution quite similar to that predicted by the asymptotic wave function. This is a result of it being a solution of the light-cone Hamiltonian for a $|q\bar{q}\rangle$ system that conserves angular momentum. Other non-perturbative wave functions such as that derived from a harmonic oscillator potential do not have this property. The agreement of the predicted u-distrubution with the E791 data [13] is not as good as that of the asymptotic wave function, but this is not surprising as these data were taken in a k_t-region that is in the $k_\perp$ tail of this function.

The non-relativistic approximation to (10) is a technical simplification but not a compelling part of the model. It can be relaxed in future work, without major difficulties.

In general, we can note that the $k_\perp$-distribution is a powerful tool for studying wave functions in the perturbative regime and in the transition region between the perturbative and non-perturbative regimes.

The data of E791 were taken more than ten years ago. With realistic light-cone wave functions now existing or coming up in the foreseeable future, dedicated diffraction experiments, possibly extended to kaons and other hadrons, should be very valuable.

References

1. S.J. Brodsky, D.S. Hwang, B.Q. Ma, I. Schmidt, Nucl. Phys. B **593**, 311 (2001)
2. S.J. Brodsky, SLAC-PUB-7870; hep-ph/9807212
3. A.H. Mueller, Nucl. Phys. B **415**, 373 (1994)
4. F. Antonuccio, S.J. Brodsky, S. Dalley, Phys. Lett. B **412**, 104 (1997)
5. S.J. Brodsky, H.C. Pauli, S.S. Pinsky, Phys. Rep. **301**, 299 (1998)
6. S. Dalley, Nucl. Phys. B (Proc. Suppl.) **90**, 227 (2000)
7. G.P. Lepage, S.J. Brodsky, Phys. Rev. D **22**, 2157 (1980)
8. S.J. Brodsky, G.P. Lepage, Phys. Scripta **23**, 945 (1981)
9. S.J. Brodsky, Springer Tracts in Modern Physics **100**, 81 (1982)
10. A.V. Efremov, A.V. Radyushkin, Theor. Math. Phys. **42**, 97 (1980)
11. G. Bertsch, S.J. Brodsky, A.S. Goldhaber, J. Gunion, Phys. Rev. Lett. **47**, 297 (1981)
12. V.L. Chernyak, A.R. Zhitnitsky, Phys. Rep. **112**, 173 (1984)
13. E791 Collaboration, E.M. Aitala et al., Phys. Rev. Lett. **86**, 4768 (2001)
14. R. Jakob, P. Kroll, Phys. Lett. B **315**, 463 (1993)
15. H.C. Pauli, Nucl. Phys. B (Proc. Supp.) **90**, 154 (2000)
16. H.C. Pauli, A. Mukherjee, Int. J. Mod. Phys. A **16**, 4351 (2001)
17. H.C. Pauli, Nucl. Phys. A **705**, 73 (2002)
18. G. Sterman, P. Stoler, Ann. Rev. Nuc. Part. Sci. **43**, 193 (1997)
19. S.J. Brodsky, G.R. Farrar, Phys. Rev. Lett. **31**, 1153 (1973)
20. L.L. Frankfurt, G.A. Miller, M. Strikman, Phys. Lett. B **304**, 1 (1993)